Geologica Acta, Vol.13, Nº 3, September 2015, 243-254
DOI: 10.1344/GeologicaActa2015.13.3.6

A new limit for the NW Río de la Plata Craton Border at about 24ºS (Argentina) detected by Magnetotellurics

A. FAVETTO[1] V. ROCHA[2] C. POMPOSIELLO[1] R. GARCÍA[2] H. BARCELONA[1]

[1]CONICET, INGEIS, Ciudad Universitaria
1428 Buenos Aires, Argentina

[2]Universidad Nacional de Salta, Hidrogeología
Salta, Argentina

ABSTRACT

Old South American structures constitute a puzzle where the Río de la Plata Craton is the most important clue in the assembly of SW Gondwana. The present study is aimed at characterizing the western border of the Río de la Plata Craton on the basis of magnetotelluric studies. Magnetotelluric (MT) data were acquired along an approximately NW-SE 750km profile at about 24ºS, from the Sub-Andean Ranges in the province of Salta (NW) to the Formosa Province frontier (SE) next to Paraguay River. Distortion and structure dimensionality analysis indicates that MT responses are two-dimensional with a NS strike orientation, consistent with the regional geological strike. A 2-D inversion of the data provided a model showing a lateral discontinuity, possibly associated with cratonic structures. The high resistivity observed (>5000ohm·m), from about the middle of the profile toward its eastern end, may be interpreted as the terranes accreted to the Río de la Plata Craton during Neoproterozoic to Cambrian times, or as the Río de la Plata Craton itself. Along the profile from the surface to a depth of about 10km the resistivity model shows a significant resistivity variation in the structure. The resistive block identified at the western end of the profile represents the Sub-Andean system. The markedly enhanced low-resistivity structure (~1 to 10ohm·m) corresponds to a sedimentary pile whose thickness decreases from NW to SE.

KEYWORDS **Magnetotelluric. Río de la Plata Craton. North Argentina. Formosa.**

INTRODUCTION

The Río de la Plata Craton (RPC) is the oldest and the southernmost Precambrian unit in South America and it is placed at the core of SW Gondwana in most of the paleogeographic reconstructions (Cordani *et al.*, 2003; Tohver *et al.*, 2006; Trindade *et al.*, 2006). The Transbrasilian Lineament (TB) is a continental scale suture between the Amazonian Craton and the São Francisco Craton and the Paraná Block (Fig. 1). Many authors inferred that the western border of the RPC could be the southern continuation of the TB in the Chaco-Pampean Plain. It defines the tectonic boundary between the RPC and the Pampean Terrane (PT) (see *e.g.*, Kröner and Cordani, 2003; Feng *et al.*, 2004; Ramos *et al.*, 2010).

It is hard to identify the RPC by direct observations and deep drilling because it is mostly covered by a very thick sediment pile. However, geophysical and deep bore-hole geochronological studies indicate that the western edge of this craton is in sharp contact with the early Paleozoic eastern Pampean Ranges (Booker *et al.*, 2004; Rapela *et al.*, 2007).

The magnetotelluric (MT) method is an effective and complementary technique to determine lithospheric

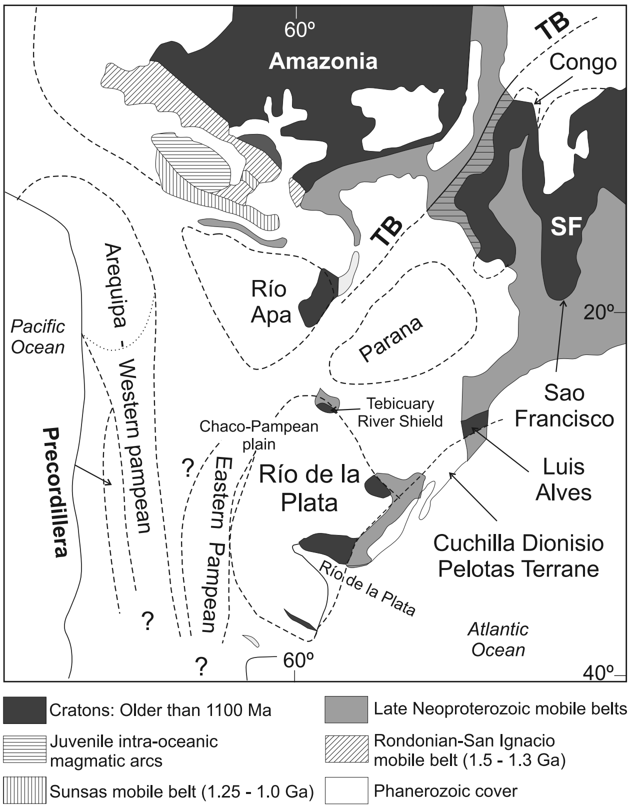

FIGURE 1. Precambrian tectonic framework in central South America (modified from Kröner and Cordani, 2003; Cordani *et al.*, 2003). Dashed lines indicate inferred boundaries of major crustal units beneath Phanerozoic cover. TB = Transbrasilian Lineament. (Modified from Rapela *et al.*, 2007).

electrical structures beneath thick sedimentary basins and it has been used in many cratonic areas (*e.g.*, the Slave Craton in northern Canada (Jones *et al.*, 2003), the Kaapvaal Craton in Southern Africa (Evans *et al.*, 2011) and the Amazonian Craton in Brazil (Bologna *et al.*, 2013).

MT and gravimetric studies in Córdoba province revealed the presence of crustal discontinuities. They are interpreted as the boundary between the RPC and the PT which might correspond to the Early Cambrian suture (Booker *et al.*, 2004; Favetto *et al.*, 2008; Ramé and Miró, 2011; Burd *et al.*, 2013).

In the Chaco-Pampean Plain, four exploration wells, located in the east and center of Córdoba province, reached the crystalline basement. The ages of these igneous rocks (2.3-2.0Ga) were determined through cutting analysis, and confirmed the affinity of the Chaco-Paranaense basement with RPC outcrops in the Tandilia Belt and Uruguayan and Brazilian terranes (Rapela *et al.*, 2007). On the other hand, in Formosa province exploration wells did not reach the crystalline basement, then there is no direct evidence supporting the presence of the RPC in this zone (Russo *et al.*, 1979).

There's a discrepancy between different authors about the geometry of the northwestern boundary of the RPC. Oyhantçabal *et al.* (2010) and Rapela *et al.* (2011) reviewed the litho-stratigraphic units of the RPC, except the blocks that were accreted to the RPC during Neoproterozoic to Cambrian times (*i.e.*, the Asunción Arch in Paraguay). Furthermore, the Tebicuary River Shield (Paraguay) is considered to be the northernmost expression of the RPC (see Fig. 1) and is characterized by rocks of the lower to upper Proterozoic (Cordani *et al.*, 2001).

This paper analyzes data acquired at 18 sites along 750km over a NW-SE profile at approximately 24ºS, which extends from the Sub-Andean Ranges in Salta province to the eastern limit of the Formosa province, next to the Paraguay River (profile A in Fig. 2). This geophysical study aims to detect the craton in this zone.

PREVIOUS MAGNETOTELLURIC STUDIES APPLIED TO THE WESTERN BORDER OF THE RÍO DE LA PLATA CRATON

From 2001 to 2012, MT data were collected from 215 sites in the Pampean Ranges and Chaco-Pampean Plain. These surveys improved the understanding of processes associated with different geological environments. Some of them B, C, D and E profiles in Figure 2, allowed constraining the geometry of the western boundary of the RPC on the basis of a sharp lateral discontinuity between two high resistive blocks. This feature was interpreted as the boundary between the RPC and the PT which may correspond with the Early Cambrian suture according to MT results. The 2-D resistivity models corresponding to profiles B, C and D are showed in Figure 3.

The profile B at about 27°S crosses the western border of Las Breñas depocenter. Resistivity distribution at the crust scale indicates that to the east of the profile the highest values of resistivity assigned to the RPC were found. To the western side, a less but still highly resistive block may be correlated with the PT. These blocks are separated by an east-dipping more conductive anomaly that could be the presumed continuation of the TB not exposed in Argentina (Peri *et al.*, 2013).

The profile C, with a length of 300km, crosses the Ambargasta-Sumampa Range and the Chaco-Pampean Plain at about 29.30ºS. The model also shows highly resistive blocks at crustal depths assigned to the RPC in the east and the PT in the west. Between both blocks, the suture is identified as a more conductive zone 20km wide (recent contribution, Peri *et al.*, 2015).

The 2-D resistivity model from profile D, with a length of 450km, at approximately 31.5ºS, shows a sharp lateral discontinuity to the east of the Sierras de Córdoba suggesting suture between the RPC and the PT (Favetto *et al.*, 2008). This discontinuity agrees with the results from previous geological studies (Ramos *et al.*, 2010 and Rapela *et al.*, 2007).

The profile E and extra sites were interpreted by a 3-D model (Burd *et al.*, 2013). The slice model corresponding to San Luis province shows a high resistive block from 65ºW to the east and about 200km deep, which is interpreted as the RPC.

GEOLOGICAL BACKGROUND

West Gondwana is the part of the super continent that is represented today by South America, Arabia, Africa and West Antarctica. It has been defined on the basis of Archaean shields, cratons and cratonic fragments, intervening Mesoproterozoic and Neoproterozoic mobile belts, and outer belts of Proterozoic–Mesozoic terranes that make it up (*e.g.*, Unrug, 1997; Pankhurst *et al.*, 1998; Brito Neves *et al.*, 1999; Vaughan and Storey, 2000; Murphy *et al.*, 2004; Tohver *et al.*, 2006).

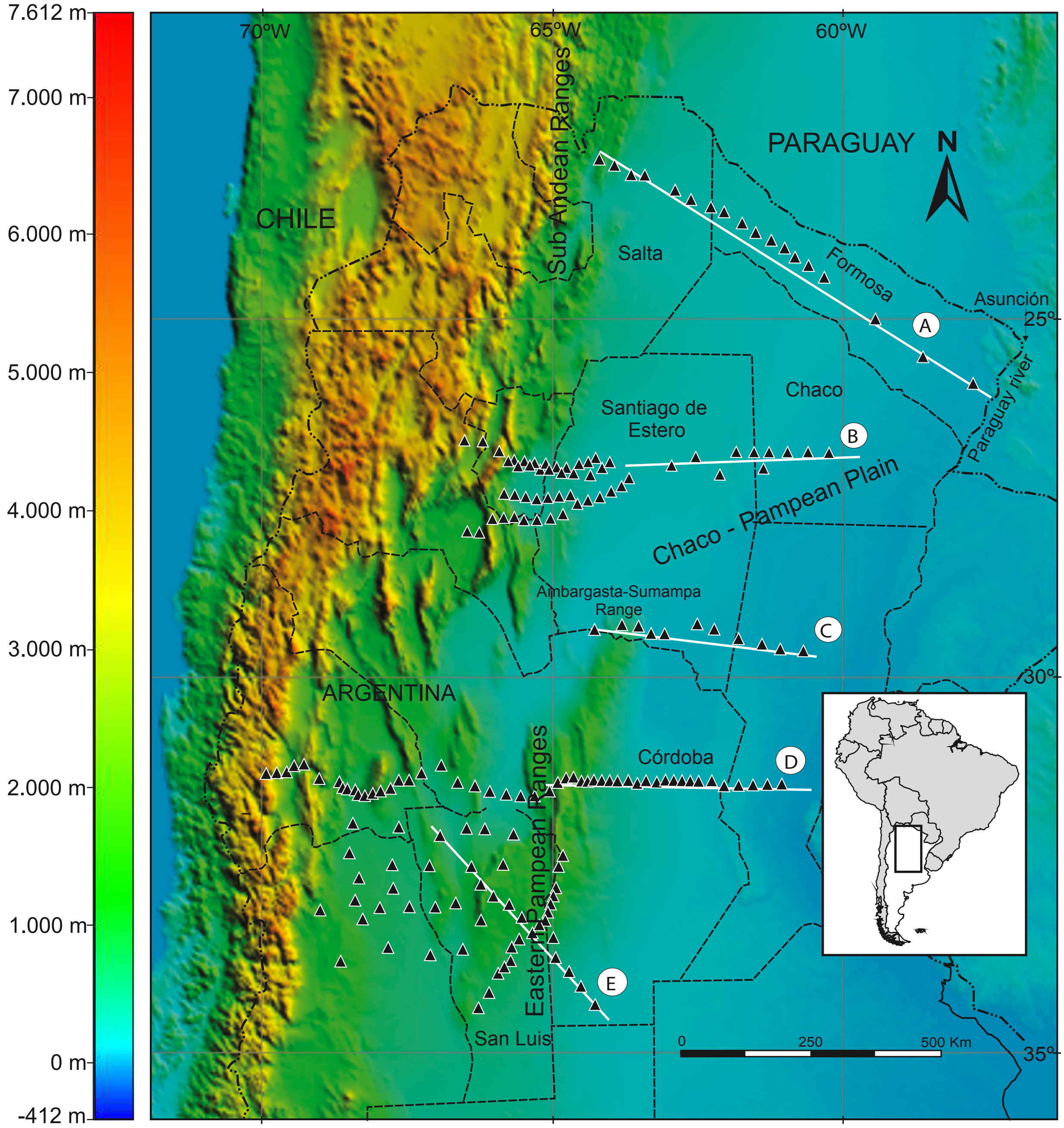

FIGURE 2. MT site locations on a digital elevation model (DEM) of South America. The black triangles are the MT sites and the white lines represent the MT profiles.

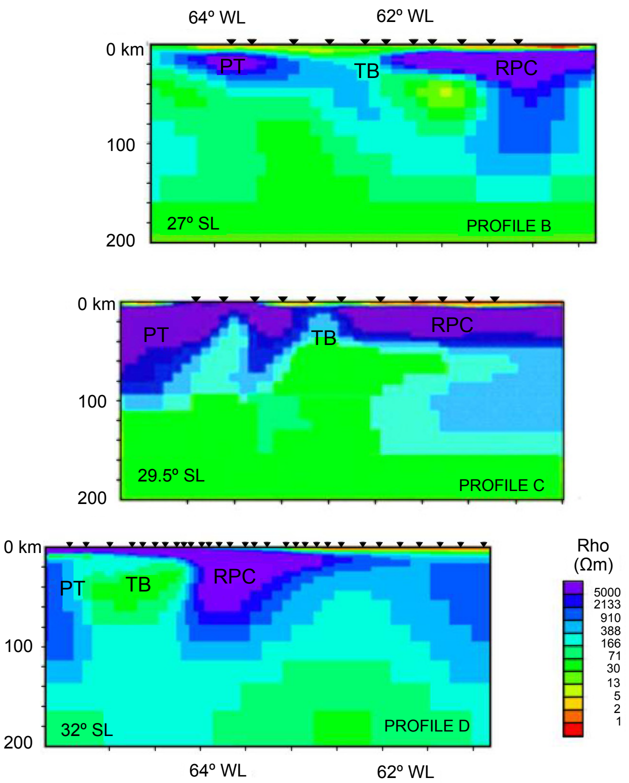

FIGURE 3. Previous 2-D resistivity models obtained by Peri *et al.* (2013) at 27ºS (profile B), by Peri *et al.* (2015) at 29.5ºS (profile C) and by Favetto *et al.* (2008) and Orozco *et al.* (2013) at 32ºS (profile D).

The most important cratons and shields are the Amazonia-West Africa Craton, São Francisco-Congo Craton, Kalahari–Grunehogna Craton, Río de la Plata Craton, and the Arabian–Nubian Shield (Tohver *et al.*, 2006). Cordani *et al.*, (2003) pointed to smaller cratonic fragments of considerable importance in understanding the evolution of the supercontinent. These include the Central Goias massif (Fischel *et al.*, 2001), and the Luiz Alves, Río Apa, São Luis and Paraná cratonic fragments (*e.g.*, Tohver *et al.*, 2006).

West Gondwana is the result of a series of accretionary and collisional events that took place across a series of Brasiliano–Pan African suture zones. The process began 850Ma ago and ended in the latest Cambrian (490Ma ago) (*e.g.*, Brito Neves *et al.*, 1999). During the final assembly stage of West Gondwana the basin between the Río de la Plata and the Amazonian cratons closed creating the Paraguai belt (Alkmim *et al.*, 2001).

Paleogeographic reconstructions indicate that the PT-RPC suture would have resulted from the closure of a large oceanic domain, the Goiás-Pharusian Pampean Ocean in the Early Cambrian (Cordani *et al.*, 2001; 2003; Rapalini, 2005). The PT represents the basement of most of the Pampean Ranges (Rapalini, 2005).

The study area is located in the north of the Chaco-Pampean Plain, between the Sub-Andean system, in the North of Argentina, and the Asuncion Arch, in Paraguay. The geological history of this region is complex; it presents basins and sub-basins which have evolved differently, and structural highs, affected by faulting and folding. The thick sedimentary sequence mainly consists of sand, silt and clay, and groundwater is characterized by a high salinity. The basin sediments and the geometry of the basement along the whole profile were described by a shallow MT model (Favetto *et al.*, 2010).

Assumpção *et al.* (2013) presented models of crustal thickness for South America from seismic refraction, receiver functions and surface wave tomography. They detected an anomalously thin crust (>30km) below the Chaco-Paranense Basin. A relatively high gravity anomaly found by Tassara and Echaurren (2012) and Tassara *et al.* (2006) confirms the generally thin crust east of the Altiplano–Puna plateau in the central Andes. In addition, Feng *et al.* (2004) found very low S-wave velocities in the upper mantle. Figure 4 shows S-wave velocity anomalies at 100km deep and the marks corresponding to the location of the MT array (profiles: A, B, C and D). These features can be considered an old inherited feature left after the rifting and drifting episodes related to the separation of Rodinia during the Neo-Proterozoic with the rifting of Gondwana.

MAGNETOTELLURIC INTERPRETATION

Data acquisition and analysis

MT long period data were acquired between 2009 and 2011 at 18 sites along a 750km profile. It extended from the west of Salta province across the Formosa province to its eastern border (profile A in Fig. 2).

Data were collected with long period, GPS-controlled MT systems (NIMS). The electric (Ex, Ey) and magnetic (Hx, Hy, Hz) fields were orthogonally recorded at the

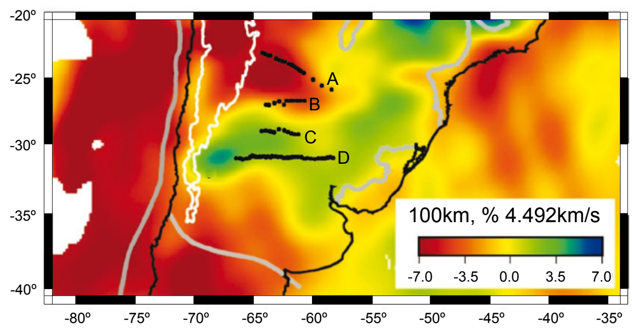

FIGURE 4. S-wave velocity anomalies at 100 km depth from Feng *et al.*, 2007. The black dots are the MT sites of the profiles A, B, C and D.

surface with axis directions defined as x to the north, y to the east and z toward the subsoil. The magnetic field was measured with "flux gate" type magnetometers in the range of 1 to 10000s. The electric field was measured with pairs of Pb–$PbCl_2$ electrodes at a distance of around 100m. Three sites were added at the eastern end of the NIMS profile. These data were obtained by Garcia *et al.*, 2008 using two commercial wideband MT receivers (EMI -MT24) synchronously to facilitate remote reference noise cancellation in the so-called dead band around 1Hz. Data were processed using robust statistical time series analysis and the remote reference multi-site method (Egbert, 1997).

Dimensionality and distortions

A discussion on "decomposition" techniques can be found, for example, in Bahr (1988, 1991), Groom and Bailey (1989), Groom *et al.* (1993), Chave and Smith (1994), Smith (1995), or McNeice and Jones (2001). These methods are often u$f$sed to determine the correct strike angle of 2-D structures in presence of local heterogeneities and distorted parameters (shear and twist).

Caldwell *et al.* (2004) introduced a method that is now widely used to recognize the dimensionality of data defining a phase tensor Φ as $\Phi=X^{-1}Y$ from the complex impedance tensor Z=X+iY. In the presence of galvanic distortion the measured and regional phase tensor are identical. So, they are independent of galvanic distortion. The graphic representation of the phase tensor (and in fact of any 2 2 real matrix) is an ellipse. An invariant parameter of this tensor is the skew angle defined as:

$$Skew\ angle = \frac{1}{2} \cdot \tan -1\left((\phi_{12} - \phi_{21})/(\phi_{11} + \phi\varphi_{22})\right)$$

The phase tensor determines whether the 2-D structure approximation is valid when its absolute value is less than 1.5º (Bibby *et al.*, 2005).

Another useful invariant, called ellipticity (λ) determines that the symmetry of the structure may be assumed to be 1-D when it is smaller than 0.1. It is defined as:

$$\lambda = \left((\phi_{max} - \phi_{min})/(\phi_{max} + \phi_{min})\right)$$

In this paper the dimensionality of electrical conductivity was analyzed using the skew angle from phase tensor analysis (Caldwell *et al.*, 2004; Bibby *et al.*, 2005). The best geoelectrical strike and the distorted parameters were determined using multi-site and multi-frequency tensor decomposition (McNeice and Jones, 2001).

Figure 5 shows the ellipticity, phase tensor skew angle and azimuth of phase tensor maximum (orientation of the major axis which coincides with the geoelectrical strike in the 2-D situation) for a site that can be considered representative of the average behavior of all sites (for40). Ellipticity values below 0.1 for periods shorter than 30s, indicate a 1-D structure for shallow depths. For periods longer than 30s the phase tensor skew angle is around ±3.0º, showing that the structure can be considered 2-D. The bottom panel in Figure 5 shows that the phase tensor maximum azimuth is close to 0º, therefore a NS regional strike can be adopted.

The phase tensor ellipses obtained for all sites (measured with NIMS systems) at all periods are in Figure 6. In general, at short periods, the ellipses are more circular which corresponds with a 1-D medium. The phase tensor skew angle is smaller than ±3º in most of the sites. So, the assumption of a 2-D regional structure can be used.

A multi-site, multi-frequency tensor decomposition developed by McNeice and Jones (2001), which is an extension to Groom-Bailey decomposition (1989), was also performed in this study. A global minimum is sought to determine the most appropriate strike direction and telluric distortion parameters for a range of frequencies and all the sites. The regional strike was determined for a period band (30–6000s) considering an error floor of 5% applied to the real and imaginary parts of the impedance tensor components. The minimum period selected was 30s because at most sites the shallow structure can be considered 1-D. The processing of all the sites together gave strike values of 1.33ºNE. In Figure 7 the distorted parameters (twist and shear) and normalized RMS misfits are presented. These parameters are descriptors of the degree of distortion of deeper structures by electric charges that form on very small-scale 3-D features in the very shallow Earth.

In general, twist and shear values are smaller than ±10º and the normalized RMS error are around 2. Exceptional

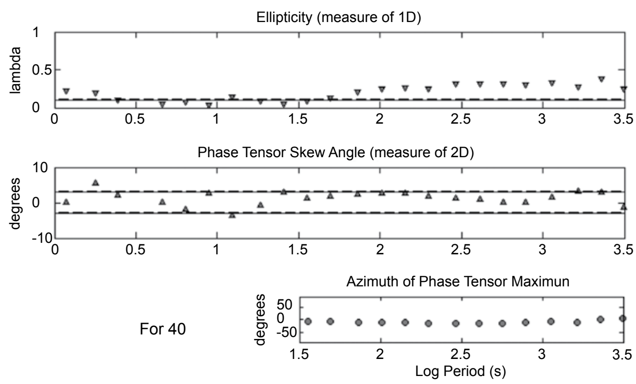

FIGURE 5. Variation of dimensional parameters with period: ellipticity, phase tensor skew angle and azimuth of phase tensor maximum for MT site for40, shown as an example.

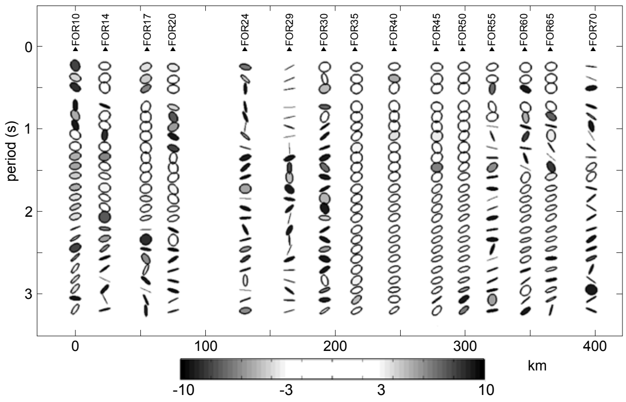

FIGURE 6. Phase tensor ellipses for all sites (measured with NIMS systems) at all periods, gray scale represents the phase tensor skew angle. Ellipses are plotted so that the horizontal axis corresponds to the NW-SE direction.

distortion was observed at sites for24, for29 and for55 where the shear is larger, around ±20º. Twist values are small except at sites for17, for24 and for55. These results are consistent with those observed in the phase tensor analysis (Fig. 6). The NRMS is low enough for a 2-D assumption to be considered as a good representation of the structure. Distortions can be considered weak.

The data obtained with broadband systems can be considered 1-D for periods less than 10s and 2-D for the range 10s to 300s.

2-D MT model

For 2-D structures, data can be separated into two independent modes with electric current flowing parallel (TE) and perpendicular (TM) to the approximately NS strike direction. Pseudo-sections of apparent resistivity (r) and phase (f) for both polarizations are shown in Figure 8 for the period range of 4–4000s and real and imaginary parts of the transfer function between vertical and horizontal magnetic field (Tzy) in measurement coordinates are shown in Figure 8 for the same period range.

MT data were inverted using the NLCG algorithm of Rodi and Mackie (2001). Usually, apparent resistivities and phases in both polarizations, TE (r_{xy},f_{xy}) and TM (r_{yx},f_{yx}), and Tzy can be also inverted using this algorithm. Inversion minimizes model roughness subject to fitting the data to a prescribed error.

The starting half space resistivity of 1000ohm·m was used. When the normalized root mean square (NRMS) of the inversion was about 1.6 and t was 10, the model was achieved. Modes, TE and TM, and Tzy were inverted jointly, setting data error floors of 10% in TM (r_{yx}), and TE (r_{xy}), 2.9 degrees in the phases (f_{yx} and f_{xy}) and 0.03 in Tzy. The final model is presented in Figure 9.

From the surface to a depth of about 10km the shallow model shows significant structure variation. At the western end of the profile, the Sub-Andean system is represented by a resistive block (>500ohm·m), which indicates the western edge of the sedimentary basin. Very low resistivity ranging from 1 to 10ohm·m corresponds to sediments and the model shows that the basin is deepest in sites for17 to for29, reaching 10km (Fig. 9).

The deep model shows a lateral discontinuity around sites for45-for55. To the west the resistivity is less than 100ohm·m and to the east a large resistivity block extends to the end of the profile up to a depth around 140km. The most resistive block is observed from for70 to the east and up to a depth of around 50km with resistivity values exceeding 5000ohm·m. The latter structure shows significant cratonic signature and the thickness of the all sediments above was found to be about 500m, noticeably thinner than to the west.

The responses predicted by the model and the data measured are shown as pseudosections in Figure 8. A comparison between observed data and model responses indicates that this model provides a very good fit for apparent resistivity (r_{xy} and r_{yx}), phases (fyx and f_{xy}) and fyx (real and imaginary parts).

CONCLUSIONS AND DISCUSSION

As it has been mentioned above, several authors have contributed to establish the geometry of the RPC border in the Chaco-Pampean Plain. Because of the RPC is poorly exposed, its boundary has been inferred from geochronological and geophysical studies. As armed, an ongoing debate exists on the relationship between RPC and

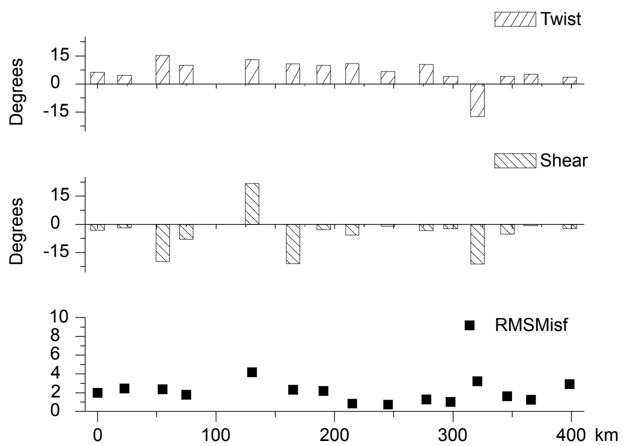

FIGURE 7. Distorted parameters (twist and shear) determined at multiple sites for a range of periods (30 – 6000s) and normalized RMS errors. This processing gave strike values of 1.33ºNE.

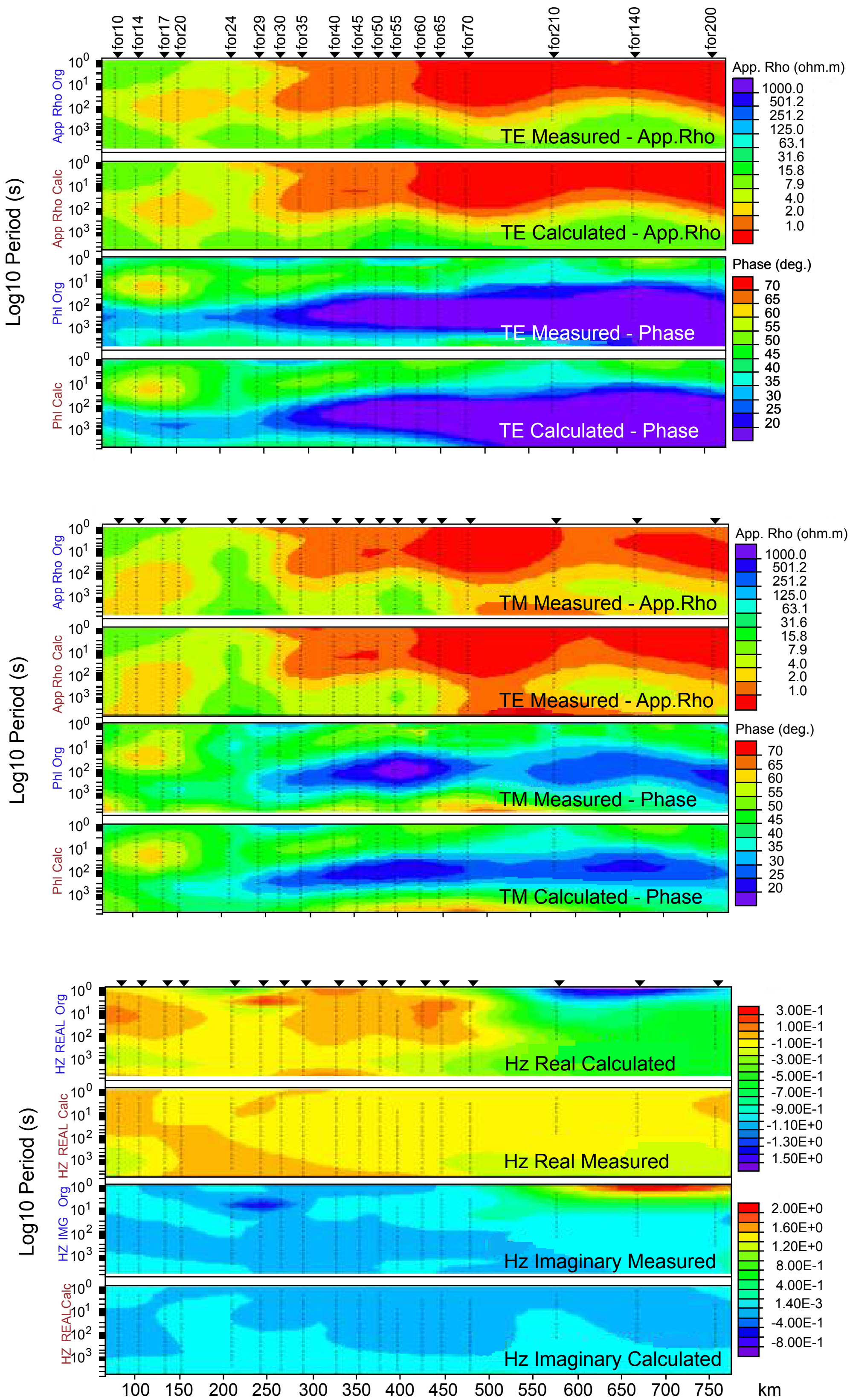

FIGURE 8. Measured MT data and calculated model response pseudosection of apparent resistivity (xy and yx expressed in ohm-m), Phase (xy and yx expressed in degrees º) and Hz (Real and Imaginary). Periods range from 4 to 4000s.

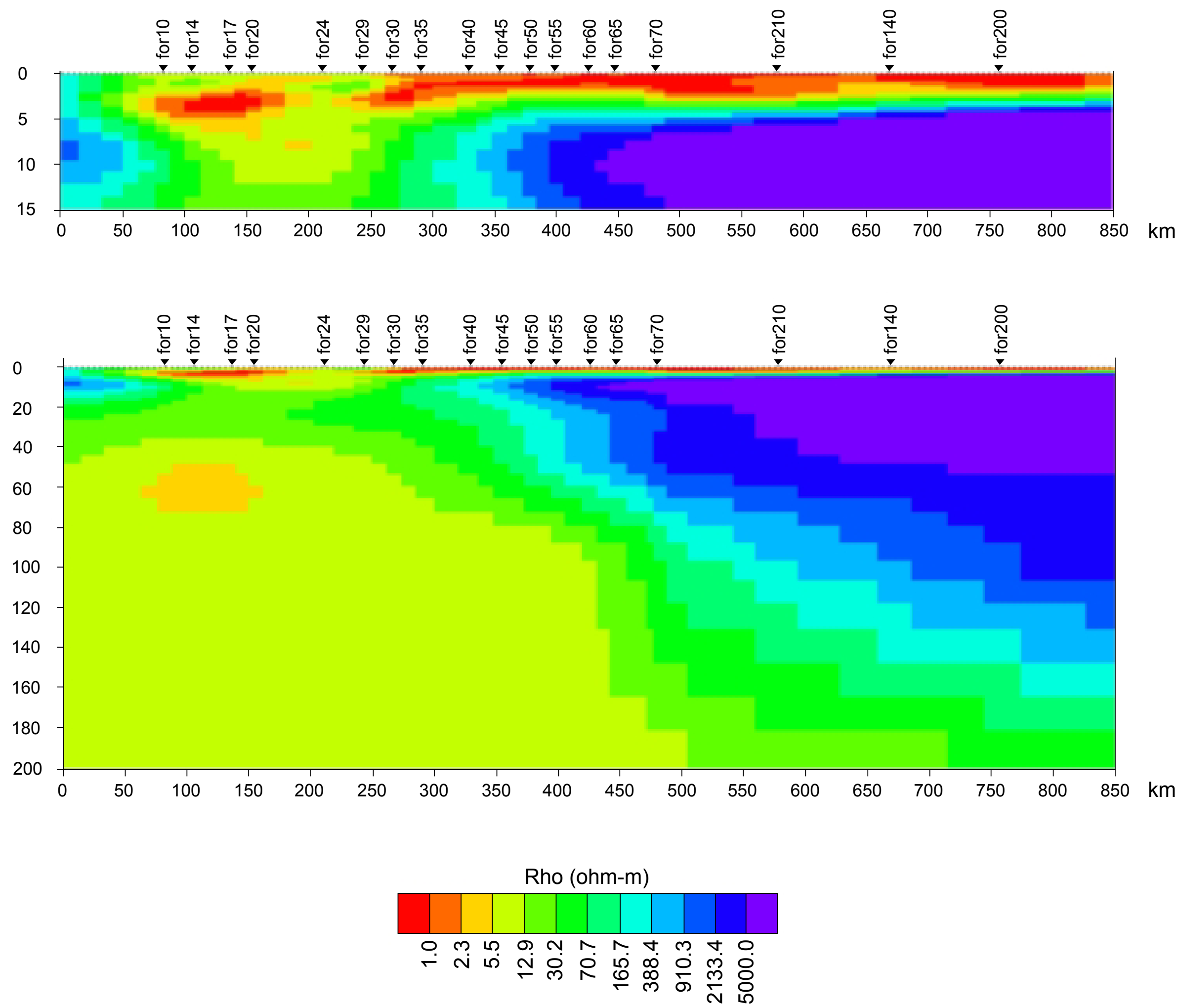

FIGURE 9. The final 2-D inversion model, NE-SW (log10 scale 1-5000 ohm·m) see profile A in Figure 2, obtained up to 200km deep and a detail of this model of the shallow part (up to 20km deep).

large neighboring morphostructural units in the northern part of the Chaco-Pampean Plain (in Chaco, Salta and Formosa Provinces).

Previous MT data, mentioned in section 2, showed information from deep structure in different sectors (from 27ºS to 34ºS) of the Chaco-Pampean Plain that was consistent with the results obtained from geological and geophysical studies in the western RPC border (Chernicoff and Zapetini, 2004; Rapela *et al.*, 2007, 2011; Ramos *et al.*, 2010; Ramé and Miró, 2011). In Figure 10 a line connects the sharp lateral discontinuity between two high resistive blocks as observed in the profiles B to E (Favetto *et al.*, 2008; Orozco *et al.*, 2013; Burd *et al.*, 2013; Peri *et al.*, 2013, 2015). This discontinuity was interpreted as the boundary between the RPC and the PT according to the limit proposed for the RPC (Rapela *et al.*, 2007) and the inferred TB (Ramos *et al.*, 2010).

This paper presents a model, for profile A, with clearly differentiated electrical resistivity sequences. In Figure 11, a block diagram shows the geological interpretation of the study area. The moho depth obtained from seismic refraction (Assumpção *et al.*, 2013) was added in the figure. The MT model indicates that the upper crust contains an upper layer with low resistivity values (1-10ohm·m) representing the sedimentary basin. In the western edge of this basin a resitivity block (>500ohm·m) is related with the Sub-Andean system.

The mid-lower crust revealed different electrical features. Below the Sub-Andean system and the sedimentary basin the resistivity value is within 30-300ohm·m. From approximately the middle of the profile to the east the resistivity is greater than 500ohm·m, including a very resistive blockwith the highest values, >5000ohm·m, at the eastern part of the profile. This high resistivity block may be a cratonic structure.

The upper-mantle revealed a conductive anomaly with a resistivity value larger than 10ohm·m. Below the cratonic structure a root with resistivity value within 500 to 2000ohm·m is observed. This feature has also been identified in profiles B and C (see Fig. 3, Peri *et al.*, 2013, 2015).

The map, of Figure 11, shows the limit for the RPC proposed by Rapela *et al.* (2007), which reveals a discrepance of about 100km relative to the interpretation MT cratonic border. Furthermore, as it has been mentioned above, in the Formosa province, the exploration wells did not reach the crystalline basement, then there is no direct evidence supporting the presence of the RPC in this zone.

Given that the northernmost evidence of the RPC is found in the Río Tebicuary Shield (Paraguay), the

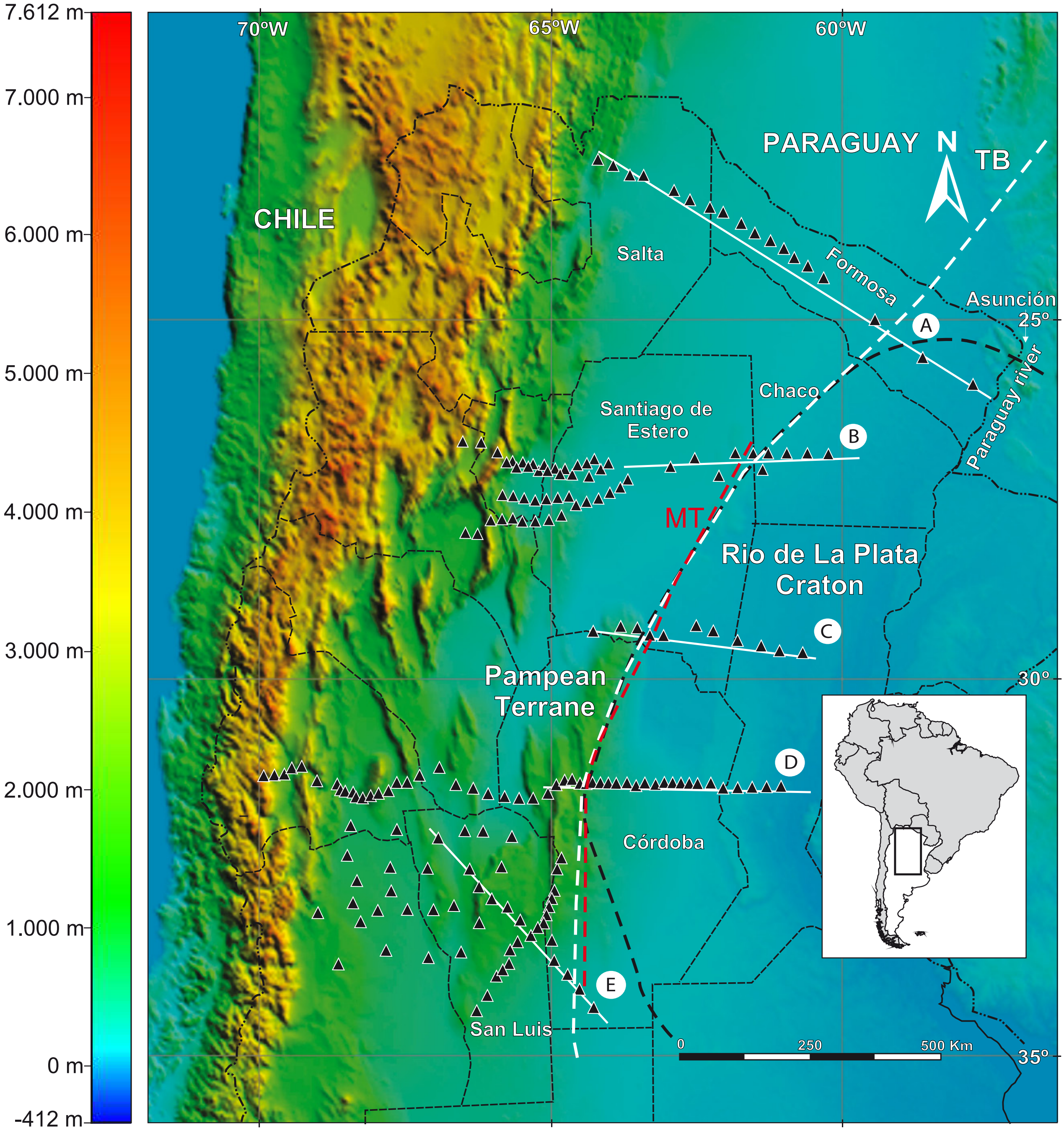

FIGURE 10. Map showing the limit proposed for the RPC (black dash line: Rapela *et al.*, 2007), the inferred TB (white dash line: Ramos *et al.*, 2010) and the sharp lateral discontinuity between two high resistive blocks in profiles B, C, D, and E. This fact was interpreted as the boundary between the RPC and the PT which may correspond the suture according to MT results.(red dash line: Favetto *et al.*, 2008, Orozco *et al.*, 2013, Peri *et al.*, 2013 and 2015 and Burd *et al.*, 2013).

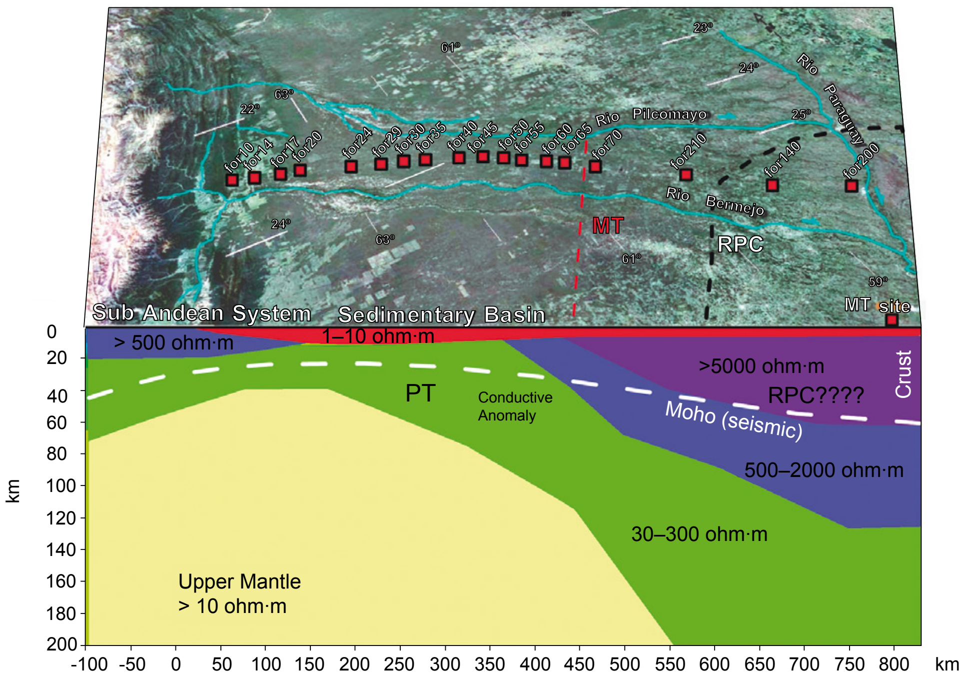

FIGURE 11. Block diagram shows the geological interpretation of the study area with MT results (red dash line).

authors suggest that the high resistivity unit found there and interpreted as cratonic, may be the RPC and the lateral discontinuity observed in the resistivity model may represent the boundary between the RPC and the PT. This could correspond to the same Early Cambrian suture which is well identified northward, along the continental scale TB. It is worth to notice that the resistivity values corresponding to PT in the previous profiles are higher than the ones obtained in the profile A. This fact seems to be related with the very low S wave velocity anomalies in the upper mantle (100km deep) observed below the profile A (Feng *et al.*, 2004) in comparison to the values observed below previous profiles (Fig. 4).

The relevance of these results are enhanced by the fact that there are no outcrops and deep geophysical studies in this zone. A tentative limit for the western border of the RPC (Fig. 11) was provided from the MT interpretation.

ACKNOWLEDGMENTS

This work was partially supported by the Project ANCyT 2007 PICT0362. We thank Dr. John Booker, Univ. of Washington, to allow us the use of NIMS temporarily. We thank too E. Llambias and G. Giordanengo for their help in the field and CONHIDRO SRL for their support in the field work.

REFERENCES

Alkmim, F.F., Marshak, S., Fonseca, M.A., 2001. Assembling West Gondwana in the Neoproterozoic: clues from the São Francisco craton region, Brazil. Geology, 29(4), 319-322.

Assumpção, M., Feng, M., Tassara, A., Julià, J., 2013. Models of Crustal Thickness for South America from Seismic Refraction, Receiver Functions and Surface Wave Tomography. Tectonophysics, 609, 82-96.

Bahr, K., 1988. Interpretation of the magnetotelluric impedance tensor: regional induction and local telluric distortion. Journal of Geophysics, 62, 119-127.

Bahr, K., 1991. Geological noise in magnetotelluric data: a classification of distortion types. Physics of the Earth and Planetary Interiors, 66(1-2), 24-38.

Bibby, H.M., Caldwell, T.G., Brown, C., 2005. Determinable and non-determinable parameters of galvanic distortion in magnetotellurics. Geophysical Journal International, 163, 915-930.

Bologna, M.S., Nunes, H.O., Padilha, A.L., Vitorello, Í., Pádua, M.B., 2013. Anomalous electrical structure in the northwestern Paraná Basin, Brazil, observed with broadband magnetotellurics. Journal South American Earth Science, 42, 74-82.

Booker, J., Favetto, A., Pomposiello, C., 2004. Low electrical resistivity associated with plunging of the Nazca flat slab beneath Argentina. Nature, 429, 399-403.

Brito Neves, B.B., Campos Neto, M.C. Fuck, R.A., 1999. From Rodinia to Western Gondwana: an approach to the Brasiliano-Pan African cycle and orogenic collage. Episodes, 22, 155-166.

Burd, A., Booker, J., Mackie, R, Pomposiello, C., Favetto, A., 2013. Electrical Conductivity of the Pampean shallow subduction region of Argentina near 33ºS: Evidence for a slab window. Geochemistry, Geophysics, Geosystems, 14(8), 3192-3209.

Chave, A.D., Smith, T., 1994. On electric and magnetic galvanic distortion tensor decompositions. Journal of Geophysical Research, 99, 4669-4682.

Caldwell, T.G., Bibby, H.M., Brown, C., 2004. The magnetotelluric phase tensor. Geophysical Journal International, 158, 457-469.

Chernicoff, C.J., Zappettini, E.O., 2004. Geophysical evidence for terrane boundaries in south-central Argentina. Gondwana Research, 7, 1105-1116.

Cordani, U.G., Brito-Neves, B.B., D'Agrella-Filho, M.S., 2001. From Rodinia to Gondwana: a review of the available evidence from South America. Gondwana Research, 4, 600-602.

Cordani, U.G., D'Agrella-Filho, M.S., Brito-Neves, B.B., Trindade, R.I.F., 2003. Tearing up Rodinia: the Neoproterozoic palaeogeography of South American cratonic fragments. Terra Nova, 15(5), 350-359.

Egbert, G.D., 1997. Robust multiple-station magnetotelluric data processing. Geophysical Journal International, 130, 475-496.

Evans, R., Jones, A., Muller, M., Hamilton, M., Evans, S., Fourie, C., Spratt, J., Webb, S., Jelsma, H., Hutchins, D., 2011. Electrical lithosphere beneath the Kaapvaal craton, southern Africa. Journal of Geophysical Research: Solid Earth, 116 B04105, 16pp.

Favetto, A., Pomposiello, C., López de Luchi, M. , Booker, J., 2008. 2D magnetotelluric interpretation of the crust electrical resistivity across the Pampean terrane-Río de la Plata suture, in central Argentina. Tectonophysics, 459, 54-65.

Favetto, A., Rocha V., Pomposiello, C., García, R., Curcio, A., 2010. Geologic features of the main crustal structures at the Chaco-Pampean Plain, Formosa Province in NW Argentina from Magnetotellurics. Electromagnetic Induction in the Earth 20th Workshop Abstract, Giza, Egypt, September 18-24, 2010.

Feng, M., Assumpção, M., Van der Lee, S., 2004. Group-velocity tomography and lithospheric S-velocity structure of the South American continent. Physics of the Earth and Planetary Interiors, 147, 315-331.

Fischel, D.P., Pimentel, M.M., Fuck, R.A., Armstrong, R., 2001. U–Pb SHRIMP and Sm–Nd geochronology of the Silvânia Volcanics and Jurubatuba Granite: juvenile Paleoproterozoic crust in the basement of the Neoproterozoic Brasília Belt, Goiás, central Brazil. Anais da Academia Brasileira de Ciências, 73, 445-460.

García, R. F., Rocha Fasola V., Moya Ruiz F. A., Tálamo, E., García Ortiz, M., Favetto, A., Pomposiello, C, J. Vargas Yegros, 2008. Hidrología Subterránea Profunda de la Provincia de Formosa. República Argentina. Modelo Geoeléctrico–Magnetotelúrico. IX Congreso ALHSUD, Quito. Ecuador.

Groom, R.W., Bailey, R.C., 1989. Decomposition of magnetotelluric impedance tensor in the presence of local three-dimensional galvanic distortion. Journal of Geophysical Research, 94, 1913-1925.

Groom, R.W., Kurtz, R.D., Jones, A.G., Boerner, D.E., 1993. A quantitative methodology to extract regional magnetotelluric impedances and determine the dimension of conductive structure. Geophysical Journal International, 115(3), 1095-1118.

Jones, A.G., Lezaeta, P., Ferguson, I.J., Chave, A.D., Evans, R.L., Garcia, X., Spratt, J., 2003. The electrical structure of the Slave craton. Lithos, 71, 505-527

Kröner, A., Cordani, U.G., 2003. African, southern Indian and South American cratons were not part of the Rodinia supercontinent: evidence from field relationships and geochronology. Tectonophysics, 375(1-4), 325-352.

McNeice, G.W., Jones, A.G., 2001. Multisite, multifrequency tensor decomposition of magnetotelluric data. Geophysics, 66, 158-173.

Murphy, J.B., Pisarevsky, S.A., Nance, R.D., Keppie, J.D., 2004. Neoprotero-zoic–Early Paleozoic evolution of peri-Gondwanan terranes: implications for Laurentia–Gondwana connections. International Journal of Earth Sciences, 93, 659-682.

Orozco, L.A., Favetto, A., Pomposiello, C., Rossello, E. Booker, J., 2013. Crustal deformation of the Andean foreland at 31°30'S (Argentina) constrained by magnetotelluric survey. Tectonophysics, 582, 126-139.

Oyhantçabal, P., Siegesmund, S., Wemmer, K., 2010. The Río de la Plata Craton: a review of units, boundaries, ages and isotopic signature. International Journal of Earth Science, 100, 201-220.

Pankhurst, R.J., Weaver, S.D., Bradshaw, J.D., Storey, B.C., Ireland, T.R., 1998. Geochronology and geochemistry of pre-Jurassic superterranes in Marie Byrd Land, Antarctica. Journal of Geophysical Research, 103, 2529-2547.

Peri, V.G., Pomposiello, M.C., Favetto, A., Barcelona, H., Rossello, E., 2013. Magnetotelluric evidence of the tectonic boundary between the Río de La Plata Craton and the Pampean Terrane (Chaco-Pampean Plain, Argentina): the extension of the Transbrasilian Lineament. Tectonophysics, 608, 685-699.

Peri, V.G., Barcelona, H., Pomposiello, M.C., Favetto, A., 2015. Magnetotelluric characterization through the Ambargasta-Sumampa Range: The connection between the northern and southern trace of the Río de La Plata Craton-Pampean Terrane tectonic boundary. Tectonophysics, 59, 1-12.

Ramé, G.A., Miró, R.C., 2011. Modelo geofísico de contacto entre el Orógeno Pampeano y el Cratón del Río de La Plata en las provincias de Córdoba y Santiago del Estero. Serie Correlación Geológica 27(2), 111-123.

Ramos, V.A., Vujovich, G., Martino, R., Otamendi, J., 2010. Pampia: A large cratonic block missing in the Rodinia supercontinent. Journal of Geodynamics, 50, 243-255.

Rapalini, A.E., 2005. The accretionary history of southern South America from the latest Proterozoic to the late Paleozoic: some paleomagnetic constraints. Geological Society, London (Special Publication) 246, 305-328.

Rapela, C.W., Pankhurst, R.J., Casquet, C., Fanning, C.M., Baldo, E.G., González-Casado, J.M., Galindo, C., Dahlquist, J., 2007. The Río de la Plata craton and the assembly of SW Gondwana. Earth Science Reviews, 83(1-2), 49-82.

Rapela, C.W., Fanning, C.M., Casquet, C., Pankhurst, R.J., Spalletti, L., Poiré, D., Baldo, E.G., 2011. The Río de la Plata craton and the adjoining Pan-African/brasiliano terranes: Their origins and incorporation into south-west Gondwana. Gondwana Research, 20, 673-690.

Rodi, W., Mackie, R.L., 2001. Nonlinear conjugate gradients algorithm for 2D magnetotelluric inversion. Geophysics, 66(1), 174-187.

Russo, A., Ferrelo, R., Chebli, G., 1979. Llanura Chaco Pampeana. Segundo Simposio de Geología Regional Argentina. Academia Nacional de Ciencias. Volumen I. Córdoba.

Smith. J.T., 1995. Understanding telluric distortion matrices. Geophysical Journal International, 122, 219-226.

Tassara, A., Echaurren, A., 2012. Anatomy of the Andean subduction zone: three dimensional density model upgraded and compared against global-scale models. Geophysical Journal International, 189(1), 161-168.

Tassara, A., Götze, H.-J., Schmidt, S., Hackney, R., 2006. Three-dimensional density model of the Nazca plate and the Andean continental margin. Journal of Geophysical Research, 111, B09404.

Tohver, E., D'Agrella-Filho, M.S., Trindade, R.I.F., 2006. Paleomagnetic record of Africa and South America for the 1200–500Ma interval and evaluation of Rodinia and Gondwana assemblies. Precambrian Research, 147(3), 193-222.

Trindade, R.I.F., D'Agrella-Filho, M.S., Epof, I., Brito-Neves, B.B., 2006. Paleomagnetism of the early Cambrian Itabaiana mafic dikes, NE Brazil, and implications for the final assembly of Gondwana and its proximity to Laurentia. Earth and Planetary Science Letters, 244, 361-377.

Unrug, R., 1997. Rodinia to Gondwana: the geodynamic map of Gondwana supercontinent assembly. GSA Today, 7, 1-6.

Vaughan, A.P.M., Storey, B.C., 2000. The eastern Palmer Land shear zone: a new terrane accretion model for the Mesozoic development of the Antarctic Peninsula. Journal of the Geological Society (London), 157, 1243-1256.

Manuscript received July 2014;
revision accepted June 2015;
published Online July 2015.